Experimental Analysis and Modeling of Single-Sided vs Dual-Sided Filtering in Flex-Grid Switched Optical Networks

Experimental Analysis and Modeling of Single-Sided vs Dual-Sided Filtering in Flex-Grid Switched Optical Networks

1st Emanuele Virgillito
Politecnico di Torino, Turin, Italy
emanuele.virgillito@polito.it

2nd Stefano Straullu
LINKS Foundation, Turin, Italy

3rd Andrea Castoldi
SM-Optics, Cologno Monzese, Italy

4th Giuseppe Parisi
SM-Optics, Cologno Monzese, Italy

3th Fransisco M. Rodriguez
SM-Optics, Cologno Monzese, Italy

3th Andrea Bovio
SM-Optics, Cologno Monzese, Italy

3th Rosanna Pastorelli
SM-Optics, Cologno Monzese, Italy

7th Vittorio Curri
Politecnico di Torino, Turin, Italy

***Abstract*—Flex-grid WSS filters embedded in Reconfigurable Add-Drop Multiplexers (ROADM) can selectively filter portions of the spectrum down to the GHz granularity enabling flexibility in optical channel add-drop operations. In this scenario, the signal's quality of transmission (QoT) can be severely impaired due to filters cascade by both single-sided (SS) and dual-sided (DS) passband narrowing, due to filters' deviation from nominal frequency or multi-carrier transceivers switching. We experimentally observe lower penalties in the SS filtering case and their interplay w.r.t. ASE noise placement. We also propose an experimental calibration method able to directly estimate the overall signal QoT degradation suitable to integration in digital twins' lightpath computation engines and network planners.**

I. Introduction

The growth of 5G, cloud services, and online applications has led to a significant increase in Internet traffic, particularly in metropolitan areas. To meet such growing demand, metropolitan optical networks are adopting coherent optical technologies and switched architectures based on reconfigurable add/drop multiplexers (ROADMs) which integrate wavelength selective switches (WSS)s to filter and route lightpaths towards different directions. The standardization of coherent technology based on digital signal processing (DSP) transceivers (TRX) as open pluggable interfaces with bit rates up to 400G and farther has made it crucial to compute the path feasibility over transparent lightpaths, even in metropolitan scenarios. In core networks, the approximation of lightpaths as affected by the amplified spontaneous emission (ASE) noise and non-linear interference (NLI) can be accurately modeled using the generalized signal-to-noise ratio (GSNR) [1]. While these two sources of impairment have been widely investigated, less attention has been paid to the issues arising from optical routing, especially with respect to the filtering effects induced by ROADM's WSSs. Indeed, metropolitan meshed networks may have several switching sites across the lightpath and less ASE noise added due to shorter distances, so the filtering degradation due to the WSS cascaded effect must be considered within the lightpath computation engine (L-PCE), as they may lead to significant signal quality degradation. Such degradation is caused by the progressive spectral narrowing on the signal spectrum sides [5] resulting from the multiplication of the cascaded WSS filters transfer functions, as outlined in Fig.1 which reports a typical flex-grid scenario in a ring topology where a channel under test (CuT) passes several nodes. Furthermore, this effect has been mostly studied in the form of double-sided (DS) filtering, a passband narrowing where the optical CuT is evenly filtered on both sides of its spectrum, as shown in Fig.2, being the most common filtering effect in the fixed-grid era [4], [8], [10]. However, modern flex-

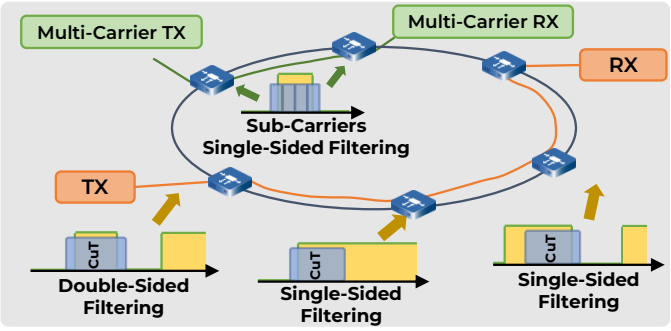

Fig. 1: Representation of the Flex-bandwidth management that can make High-Pass effects relevant for a network channel

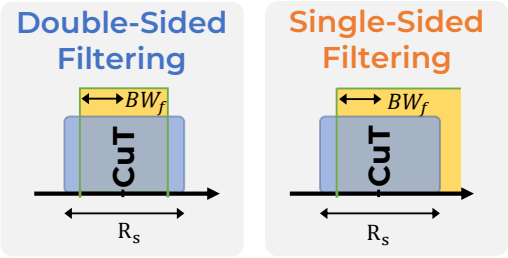

Fig. 2: Band-Pass and High-Pass filter characteristics and definition of filter bandwidth BW_f

978-3-903176-62-1 © 2024 IFIP

grid optical networks employ ROADMs whose WSS filters bandwidth can be tuned with a typical granularity of 6.25 GHz to allow optical channels' routing with different symbol rates (from 32 GBaud to 64 or 128 Gbaud) or even larger spectral portions composed of more than one Wavelength Division Multiplexing (WDM) channels. In this scenario, the side channels in the selected spectrum may experience single-sided (SS) filtering on one spectrum side only (Fig.2). The same effect also applies to multi-carrier transceivers [15], which have recently gained momentum as a mean to extend a transceiver (TRX) data rate with cheaper components without enlarging the symbol rate. Finally, SS filtering may also arise from the filter nominal central frequency drift caused by different manufacturers or fabrication imperfections, which also add some degree of randomization to the overall cascaded effect. Filtering penalty has been investigated in literature and the mechanism impairing the overall SNR is known to depend on the relative distribution of ASE and filters along the optical link [2], [4], [5], [9]. Also, (semi-)analytical models have been proposed to estimate the SNR degradation caused by filter cascade [2]–[4]. However, most of them have considered only the DS filter response and less experimental results and modeling trials have been considered SS filtering [13], especially jointly with its dependance on the ASE noise placement, to our knowledge. WSS filtering cuts the channel's high frequency components thus inducing intersymbol interference (ISI) which is then recovered by the adaptive equalizer stage in the digital signal processing (DSP)-based coherent receiver, so that the overall SNR penalty is heavily dependent on the DSP implementation. Being able to estimate the filtering quality of transmission (QoT) penalty is crucial in the network planning phase and in the L-PCE for configuration of open optical networks. To this aim, a suitable QoT estimation method must be developed, relying on a generic, conservative model or on preliminary transceiver characterization. In this paper we present the results and analysis of an experimental campaign comparing the effect of both DS and SS filtering on a single-carrier optical channel generated by a commercial 400G transceiver. We show that DS response leads to higher QoT penalty than the SS case and that existing models based on transceiver calibration as the one in [2] can be applied also to the latter case, providing insights on the dynamic of the phenomenon and its relationship to a proper knowledge of the intrinsic transceiver characteristic degradation. We also improve the transceiver calibration-based method of [2] by providing a physical layer impairment modeling background, separating the filtering effects from the line system impairments (ASE and NLI) and, especially, from the intrinsic transceiver noise [6], [7], [11], leaving the potential for further analytical modeling.

II. Experimental Setup

It is well known that the overall SNR filtering penalty depends on the relative placement of ASE noise source w.r.t. filtering sites, being the best case when all noise loading is done prior to the equivalent filter cascade (Pre-ASE) and the worst case when all the noise is moved after the equivalent filter (Post-ASE). Distributed configurations found in deployed optical systems show penalties lying in-between and can be modeled by weighting these extreme cases [3], [12]. We have built the Pre- and Post-ASE cases in our experimental setup, as reported in Fig.3. The CuT is a commercial TRX delivering 400 Gbps using DP-16-QAM at a symbol rate R_s = 62.5 GBaud. ASE noise is generated using an EDFA at constant output power, attenuated by a variable optical attenuator (VOA) to set the desired OSNR and progressively load the signal with noise to obtain the BER vs OSNR curves in various configurations. The BER is read on the TRX DSP interface, while the OSNR is measured with an optical spectrum analyzer (OSA) and reported in the R_s noise bandwidth. Filter cascade narrowing is emulated with a programmable filter for the DS case. The SS case is emulated using a bandpass filter whose bandwidth is larger than the signal and moving the filter central frequency w.r.t. the CuT so that only one side of the CuT spectrum is filtered. To fairly compare the two cases we consider the filter bandwidth normalized to the TRX symbol rate $BW_r = {}^{2BW_f}/_{R_s}$, being BW_f defined as the half-bandwidth w.r.t the filter central frequency (Fig.2). We first obtain the transceiver characteristic BER vs OSNR , i.e. the back-to-back (B2B) curve, describing the fundamental performance of the transceiver when the signal is loaded with ASE noise only. We should note however that these curves are obtained still retaining the filter but setting its bandwidth so that its larger than the signal ($1.06 < BW_r < 1.12$). We then measure the BER vs OSNR curves for progressively narrower BW_r for all the 4x filter response and ASE placement configurations, up to a maximum $BW_r = 0.66$. Narrower filtering data could have not been acquired as larger BW_r values trigger sync loss at the receiver. These results are reported in Fig.4, showing worse performance w.r.t. the (black) B2B as the filter bandwidth narrows. This is more clearly shown by looking at the OSNR penalty vs BW_r in Fig.5 The OSNR penalty at a certain BW_r is calculated as the difference between the required OSNR with filtering and the required OSNR in B2B, for a typical BER target of $BER_t = 6 \cdot 10^{-3}$. It thus reports how much the OSNR should be improved w.r.t the basic TRX performance to attain the same performance when the signal

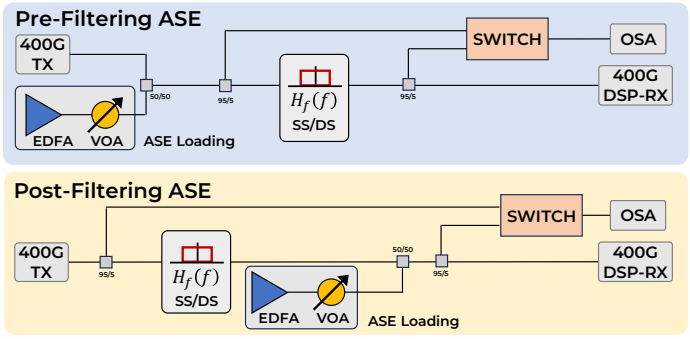

Fig. 3: Experimental setup for ASE loading placed all before (top) and all after (bottom) the filter cascade.

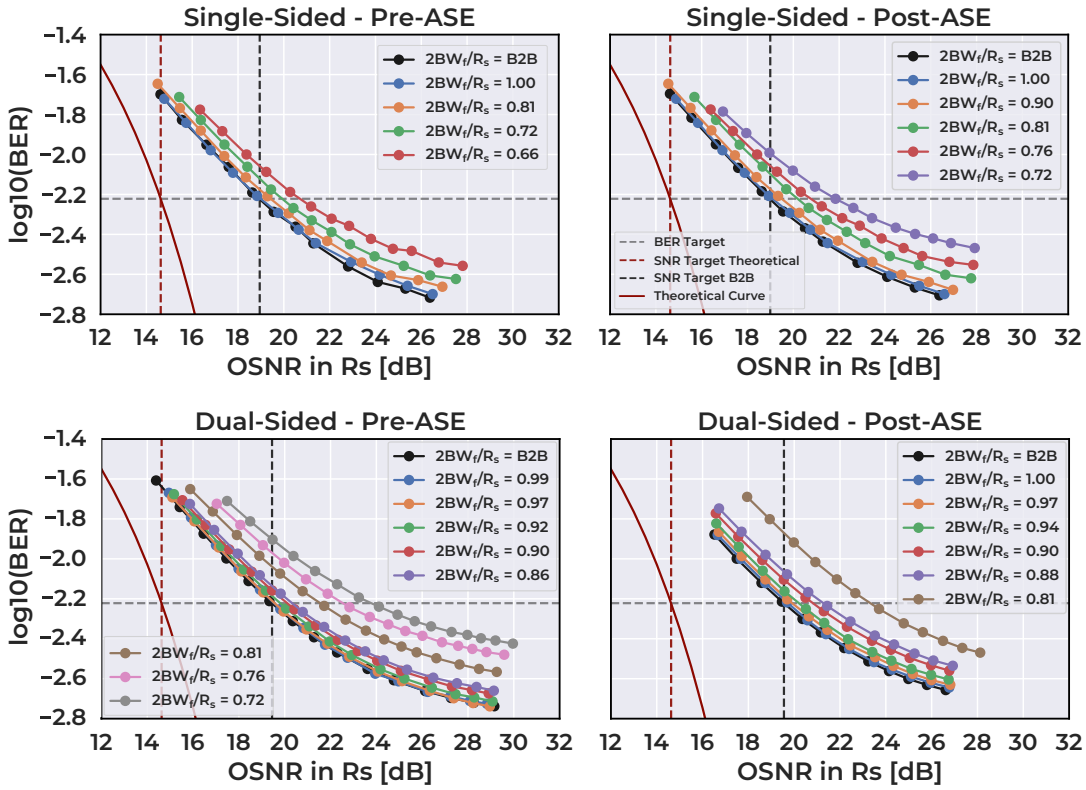

Fig. 4: Experimental BER vs OSNR curves for SS (top) and DS (bottom) filtering with Pre-ASE (left) and Post-ASE (right) configurations and tested BW_r values. All plots share the same y-axis scale. These report the experimental raw data: BER is acquired from transceiver software interface, OSNR by OSA measurement.

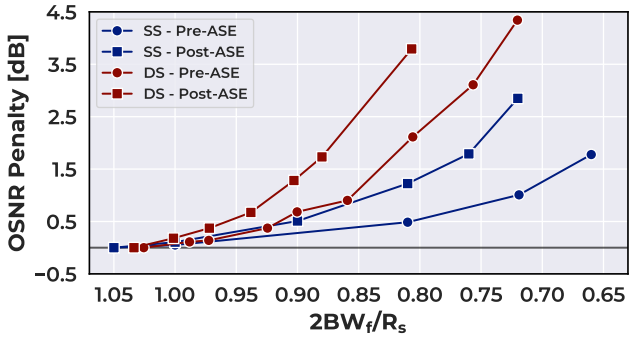

Fig. 5: OSNR penalty due to filtering effects for SS (blue) and DS (red) filtering with Pre-ASE (circles) and Post-ASE (squares) configurations at a target BER of $6 \cdot 10^{-3}$.

subdues filtering, with a peak value of 4.5 dB at $BW_r = 0.72$ for the DS, Pre-ASE scenario, while the same Post-ASE configuration has already losen the sync. As expected, for both SS and DS filtering, the Post-ASE configuration shows an additional penalty of about 1.5 dB w.r.t the Pre-ASE scenario when filtering gets significant [3], [4], [12]. Moreover, the DS filtering always delivers substantial more penalty than the SS at same BW_r, up to 3 dB in the strongest filtering case.

III. Modeling and Discussion

As previously mentioned, filter cascade cuts off high frequency components inducing ISI on the signal. In a typical DSP-receiver, the adaptive equalizer estimates the channel's frequency response and substantially implements a finite-length minimum mean-square error (MMSE) equalizer which tries to minimize the distance between the transmitted and received symbol [14]. By doing so, it balances ISI compensation (by pumping up the filtered components) and ASE noise enhancement, so that the Pre-ASE and Post-ASE performance are dependent on TRX and DSP implementation. In Pre-ASE scenario, ASE gets filtered and recovered by the equalizer together with signal. In Post-ASE, being added after filters, it gets amplified by the equalizer [2], [8]. Aside from various implementation details and DSP enhancements, the MMSE performance depend on the equalizer length [14]. In such scenarios, obtaining a general performance analytical model is not straightforward, since TRX implementation specific data is usually undisclosed by vendors, so one must rely on time consuming TRX characterization in laboratory. Another option involves a generic model neglecting implementation-specific details providing a worst case estimation for each TRX module. However, this should be carefully done because a vendor-agnostic overestimation of the Post-ASE scenario, which is by itself worst-case w.r.t realistic deployed configurations, may

lead to consider too large operational margins. We thus focus here on the first approach, while the latter deserves deeper investigation in future works which may integrate the findings of this work. The calibrated model proposed by Delezoide et al. in [2], [3] is a clever and insightful approach to the filtering penalty mechanism. We expand here the validation in a complete SS/DS and Pre-ASE/Post-ASE configurations and employing real data from commercially available TRXs instead of relying on offline processing. Moreover, we separate the transceiver noise source from the filtering effects in the perspective of developing a (semi-)analytical model for its estimation and implementation in planning and path computation tools such as GNPy [1]. In the AWGN channel model the pre-FEC BER can be estimated knowing the SNR at the receiver $\mathrm{SNR}_{\mathrm{TRX}}$ (i.e., after the equalizer) by means of erfc formulas:

$$BER = a_1 \cdot \mathrm{erfc}\left(a_2\sqrt{\mathrm{SNR}_{\mathrm{RX}}}\right) \tag{1}$$

where a_1, a_2 are coefficients depending on the modulation format. The BER vs $\mathrm{SNR}_{\mathrm{RX}}$ theoretical curve of Eq.1 has been reported in red in Fig.4. Although the x-axis reports the OSNR, w.r.t. the theoretical curve it corresponds to the $\mathrm{SNR}_{\mathrm{RX}}$, because Eq.1 assumes an ideal transceiver, so that the $\mathrm{SNR}_{\mathrm{RX}}$ for a certain BER assumes the meaning of *headroom* for any additive noise source. By looking at the B2B experimental curve (the transceiver module baseline perfomance), without any filtering we can see that it already exhibits an implementation penalty w.r.t. modulation theoretical curves of roughly 4 dB at the considered target BER. Hence, the corresponding OSNR penalty hides the TRX intrinsic noise source caused by device implementation, such as the ASE noise generated by the internal TRX amplifiers used to set the output power or the electrical noise generated by the optical frontend photodiodes [6], [11], [16]. Under these assumptions, the TRX intrinsic degradation can be modelled as a further additive noise, thus corresponding to an $\mathrm{SNR}_{\mathrm{TRX}}$ degradation. We can thus reconsider the generalized signal to noise ratio (GSNR) as the inverse sum of all the AWGN noise sources:

$$\frac{1}{\mathrm{GSNR}} = \frac{1}{\mathrm{SNR}_{\mathrm{TRX}}} + \frac{1}{\mathrm{OSNR}} \tag{2}$$

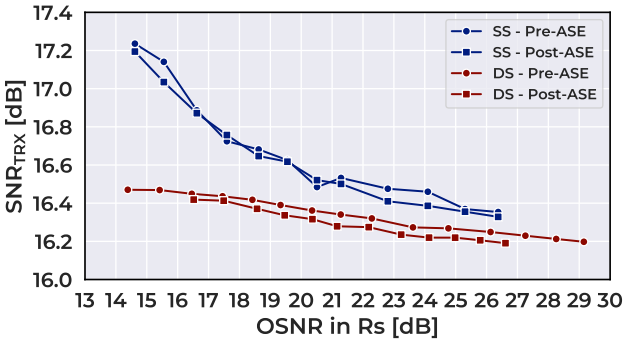

Fig. 6: Transceiver SNR $\mathrm{SNR}_{\mathrm{TRX}}$ for SS (blue) and DS (red) filtering with Pre-ASE (circles) and Post-ASE (squares) configurations extracted from the B2B experimental w.r.t. the theoretical curve.

which may also include NLI, here neglected due to absence of significant fiber propagation. In absence of filtering effects, i.e. in a pure AWGN channel, the $\mathrm{SNR}_{\mathrm{RX}}$ corresponds to the GSNR in R_s noise bandwidth. Hence, the $\mathrm{SNR}_{\mathrm{TRX}}$ can be extrapolated inverting Eq.2 from the B2B and theoretical curve of Fig.4: for each OSNR-BER couple in the B2B curve, the GSNR is thus the theoretical curve x-axis coordinate delivering the same BER. The $\mathrm{SNR}_{\mathrm{TRX}}$ is reported in Fig.6: curves with the same filter type are basically superimposed. Differences between SS and DS filtering can be attributed to the presence of a wide filter even in B2B curves. Decreasing trend with larger OSNR instead may derive from the $\mathrm{SNR}_{\mathrm{TRX}}$ dependency on total received power [11]. We can thus now consider the filtering effects: as the filter narrows the GSNR will not correspond anymore to the $\mathrm{SNR}_{\mathrm{RX}}$, but they will be related through a non-linear function $\mathrm{SNR}_{\mathrm{RX}} = \Phi\left(\mathrm{GSNR}\right)$, since filtering effect cannot be regarded as an additional noise source whilst depending on the ISI-ASE Noise balancing of the MMSE. As proposed in [2], it is expressed by means of Taylor expansion, here up to the 1st order as it can be assumed for realistic moderate filtering intensity:

$$\mathrm{SNR}_{\mathrm{RX}}{}^{-1} = \sum_{i=0}^{N} k_i \cdot \mathrm{GSNR}^{-i} \approx k_0 + k_1 \cdot \mathrm{GSNR}^{-1} \tag{3}$$

where k_0 and k_1 are the Taylor expansion coefficient up to the 1st order to be determined from experimental data. We have applied this model to the previously shown experimental data. First, we extrapolate the $(\mathrm{SNR}_{\mathrm{RX}}, \mathrm{GSNR})$ curves using the same extrapolation process used for $\mathrm{SNR}_{\mathrm{TRX}}$: for a given BW_r we obtain the BER vs GSNR curves using Eq.2. Then, the $\mathrm{SNR}_{\mathrm{RX}}$ is that one giving the same BER on the theoretical curve. The obtained values are reported with circles in Fig.7, while continuous lines are their least square method polynomial fitting obtained as in Eq.3 up to the first order. The good match between values and fitting confirms the appropriateness of the 1st order approximation also for the SS case. We then plotted the $k_{0,1}$ coefficients in dB for all the filter/placement configurations in Fig.8. k_0 represents the intrinsic TRX SNR degradation, as indeed it worsens with stronger filtering due to the equalizer limited capabilities. Curves are similar w.r.t to ASE placement with relatively small values, as the term is indeed GSNR independent. k_1 is a positive penalty enhancing the ASE noise in both SS and DS cases, reported in dB as it is actually a multiplicative factor to the AWGN noises from Eq.3. Post-ASE curves always deliver larger penalties, up to 3 dB, although in the SS case much smaller. The lower SS values can be explained as, being the signal *less filtered*, the MMSE better balances between ISI and noise enhancement.

As a last step we have tested the 1st order fit model for overall BER estimation. The proposed structure enables to estimate semi-analytically the final BER by knowing a characterization of the k_0, k_1 coefficients for the considered filter cascade and the GSNR estimation including the transceiver intrinsic degradation $\mathrm{SNR}_{\mathrm{TRX}}$, the OSNR imposed by the amplifier chain (eventually, also the NLI component). GSNR

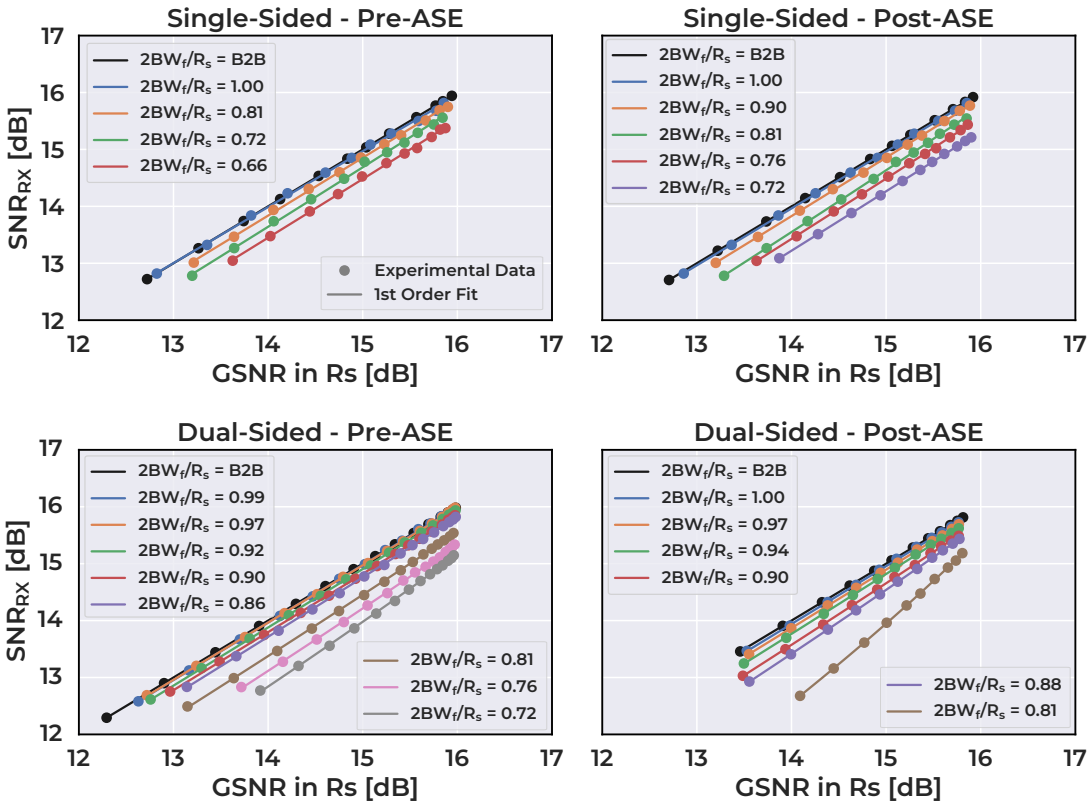

Fig. 7: GSNR vs post-equalizer $\mathrm{SNR_{RX}}$ vs normalized filter bandwidth BW_r for SS (top) and DS (bottom) filters in Pre-ASE (left) and Post-ASE (right)) configurations. Circles: measured and interpolated values. Cont. lines: 1st order least square fit. All plots share the same y-axis scale.

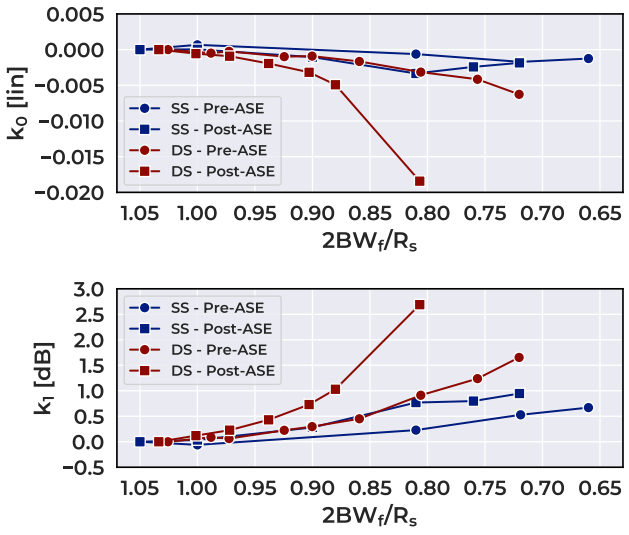

Fig. 8: Least square fit model coefficients for SS (blue) and DS (red) filtering in Pre-ASE (circles) and Post-ASE (squares): 0-th order (top plot, linear units) and 1st order (bottom plot, dB) coefficients.

is obtained using Eq.2, then the $\mathrm{SNR_{RX}}$ using Eq.3. Then, finally, the BER is given by Eq.1. Results are reported in Fig.9 for three sample values of $\mathrm{OSNR} = [18, 22, 26]$ dB, to encompass different ASE noise regimes, with circles reporting the measured values and continuous line the estimations. The 1st order fit is absolutely acccurate in all the cases, thus validating the calibration model of [3] in a realistic scenario for both extreme ASE placement scenarios and both SS and DS filtering.

IV. Conclusions

We have shown that SS filtering delivers substantially lower filtering penalty than DS filtering. We have extended the experimental validation of existing calibration models on both cases and with ASE placed before and after filters, using commercial transceiver equipment. By separating the transceiver noise contribution from the filtering effects we have proposed a solid background giving insights on the phenomenon and allowing for future modeling advancements and implementation in path computation engines. Future works will focus on fully-analytical derivations of a generic worst-case filtering penalty based on MMSE equalizer convergence.

Acknowledgment

This work has been partially funded under "Optical Access Network for 5G and beyond", grant decree 829 awarded by the Italian Ministry of Infrastructures and Made in Italy.

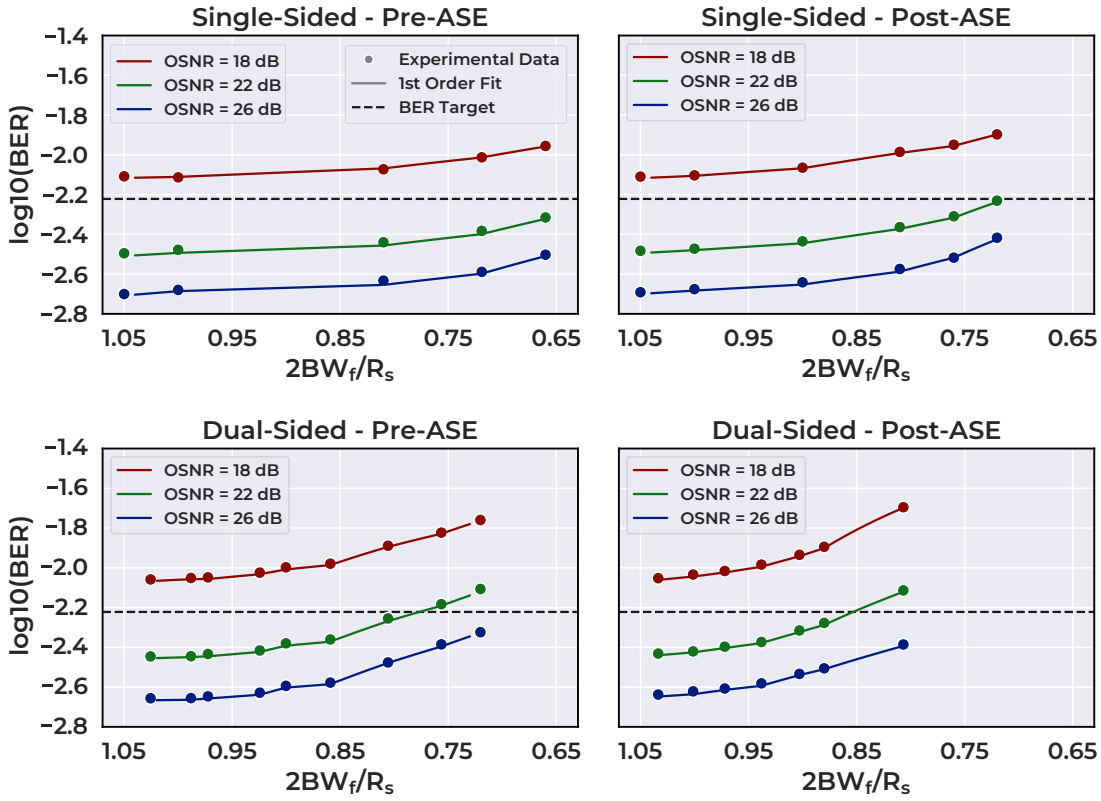

Fig. 9: BER vs normalized filter bandwidth BW_r for SS (top) and DS (bottom) filters in Pre-ASE (left) and Post-ASE (right) configurations for three sample OSNR regimes of 18, 22, 26 dB (in R_s noise bandwidth). Circles: experimental and interpolated values. Cont. lines: calibrated model estimations using the 1st order least square fit, $\mathrm{SNR}_{\mathrm{TRX}}$ estimation and BER analytical formula.

References

[1] Curri, V. GNPy Model of the Physical Layer for Open and Disaggregated Optical Networking [Invited]. *Journal Of Optical Communications And Networking*. **14**, C92-C104 (2022,6)

[2] Delezoide, C., Ramantanis, P. & Layec, P. On the Performance Prediction of Optical Transmission Systems in Presence of Filtering. *2017 19th International Conference On Transparent Optical Networks (ICTON)*. pp. 1-4 (2017,7)

[3] Delezoide, C., Ramantanis, P. & Layec, P. Weighted Filter Penalty Prediction for QoT Estimation. *2018 Optical Fiber Communications Conference And Exposition (OFC)*. pp. 1-3 (2018,3)

[4] Fernandez De Jauregui Ruiz, I., Ghazisaeidi, A., Zami, T., Louis, S. & Lavigne, B. An Accurate Model for System Performance Analysis of Optical Fibre Networks with In-line Filtering. *45th European Conference On Optical Communication (ECOC 2019)*. pp. 378 (4 pp.)-378 (4 pp.) (2019)

[5] Hsueh, Y., Stark, A., Liu, C., Detwiler, T., Tibuleac, S., Filer, M., Chang, G. & Ralph, S. Passband Narrowing and Crosstalk Impairments in ROADM-Enabled 100G DWDM Networks. *Journal Of Lightwave Technology*. **30**, 3980-3986 (2012,12)

[6] Mano, T., D'Amico, A., Virgillito, E., Borraccini, G., Huang, Y., Anazawa, K., Nishizawa, H., Wang, T., Asahi, K. & Curri, V. Modeling Transceiver BER-OSNR Characteristic for QoT Estimation in Short-Reach Systems. *2023 International Conference On Optical Network Design And Modeling (ONDM)*. pp. 1-3 (2023,5)

[7] Mano, T., D'Amico, A., Virgillito, E., Borraccini, G., Huang, Y., Kitamura, K., Anazawa, K., Masuda, A., Nishizawa, H., Wang, T., Asahi, K. & Curri, V. Accuracy of Nonlinear Interference Estimation on Launch Power Optimization in Short-Reach Systems with Field Trial. *2022 European Conference On Optical Communication (ECOC)*. pp. 1-4 (2022,9)

[8] Okamura, K., Mori, Y. & Hasegawa, H. Pre-Filtering Techniques for Spectrum Narrowing Caused by Optical Node Traversal in Ultra-Dense WDM Networks. *IEEE Photonics Journal*. **13**, 1-13 (2021,4)

[9] Pal, B., Zong, L., Burmeister, E. & Sardesai, H. Statistical Method for ROADM Cascade Penalty. *2010 Conference On Optical Fiber Communication (OFC/NFOEC), Collocated National Fiber Optic Engineers Conference*. pp. 1-3 (2010,3)

[10] Pan, J., Pulikkaseril, C., Stewart, L. & Tibuleac, S. Comparison of ROADM Filter Shape Models for Accurate Transmission Penalty Assessment. *2016 IEEE Photonics Conference (IPC)*. pp. 550-551 (2016,10)

[11] Wang, Q., Yue, Y., He, X., Vovan, A. & Anderson, J. Accurate Model to Predict Performance of Coherent Optical Transponder for High Baud Rate and Advanced Modulation Format. *Optics Express*. **26**, 12970-12984 (2018,5)

[12] Zami, T., Lavigne, B. & Cerutti, I. Filter-Induced OSNR Penalty in WDM Fiber Networks When Optical Channel Symbol Rate Grows beyond 80 GBaud. *OSA Advanced Photonics Congress (AP) 2020 (IPR, NP, NOMA, Networks, PVLED, PSC, SPPCom, SOF) (2020), Paper NeTu1B.4*. pp. NeTu1B.4 (2020,7)

[13] Searcy, S., Richter, T. & Tibuleac, S. Experimental Comparison of Single-Sided and Double-Sided Filtering in ROADM Networks. *2023 IEEE Photonics Conference (IPC)*. pp. 1-2 (2023,11)

[14] Proakis, J. Digital communications. (McGraw-Hill, Higher Education,2008)

[15] Lorences-Riesgo, A., Le Gac, D., Sales-Llopis, M., Mumtaz, S., Martins, C., De Jauregui Ruiz, I., Dris, S., Frignac, Y. & Charlet, G. Maximizing Fiber Capacity in Flex-Grid Coherent Systems Through Symbol Rate Optimization. *IEEE Photonics Technology Letters*. **34**, 161-164 (2022,2)

[16] Agrawal, G. Fiber-Optic Communication Systems. (Wiley,2021)